IN VIVO *39*: 1341-1354 (2025)
doi: 10.21873/invivo.13938

Expression of Galectin 3 and Activating Transcription Factor 3 in Nigral Dopaminergic Neurons of 6-Hydroxydopamine Induced Parkinsonian Rat Model

EUN-JIN LEE[1*], YOON-JUNG CHOY[2*], RAN-SOOK WOO[1], TAI-KYOUNG BAIK[1], HONG-IL YOO[1] and DAE-YONG SONG[1]

[1]Department of Anatomy and Neurosciences, Eulji University School of Medicine, Daejeon, Republic of Korea;
[2]Department of Optometry, Eulji University, Seongnam, Republic of Korea

Abstract

Background/Aim: Parkinson's disease (PD) is an age-related neurodegenerative disease marked by the relatively progressive dopaminergic neuronal loss in the substantia nigra (SN). Retrograde degeneration of the nigrostriatal dopaminergic neurons by 6-hydroxydopamine (6-OHDA) has been widely used as a PD animal model, while endogenous 6-OHDA promotes the progression of PD pathology. Galectin 3 (Gal3) and activating transcription factor 3 (ATF3) have been implicated in neurodegenerative processes. The aim of this study was to investigate the expression pattern and roles of Gal3 and ATF3 in a Parkinson's disease animal model induced by 6-OHDA.

Materials and Methods: We investigated temporal and spatial profiles of Gal3 expression in 6-OHDA rat model of PD. Lesions were induced by unilateral stereotactic injections of 6-OHDA into the striatum. Three days prior to 6-OHDA lesion, Fluorogold (FG) was injected at the same coordinates as the subsequent 6-OHDA injection. 6-OHDA induced retrograde degeneration of tyrosine hydroxylase immunopositive and FG immunopositive neurons within SN in a time-dependent manner.

Results: Activating transcription factor 3 (ATF3) expression was also upregulated in the SN, in a pattern similar to that of Gal3 immunoreactivity. Finally, we confirmed through triple immunofluorescence staining that ATF3 and Gal3 were colocalized in the dopaminergic neurons labeled with FG. These neurons were damaged by 6-OHDA.

Conclusion: Gal3 may play a key role in the signaling pathway of dopaminergic neuronal cell death induced by 6-OHDA. This is the first *in vivo* demonstration that Gal3 is expressed in dopaminergic neurons injured by 6-OHDA.

Keywords: Galectin 3, activating transcription factor 3, 6-hydroxydopamine, Parkinson's disease, animal model.

*These Authors equally contributed to this work.

Hong-Il Yoo, Department of Anatomy and Neurosciences, Eulji University School of Medicine, 77 Gyeryong-ro 771beon-gil, Jung-gu, Daejeon 34824, Republic of Korea. Tel: +82 422591627, Fax: +82 422591629, e-mail: hiyoo@eulji.ac.kr; Dae-Yong Song, Department of Anatomy and Neurosciences, Eulji University School of Medicine, 77 Gyeryong-ro 771beon-gil, Jung-gu, Daejeon 34824, Republic of Korea. Tel: +82 422591622, Fax: +82 422591629, e-mail:dysong@eulji.ac.kr

Received September 28, 2024 | Revised January 11, 2025 | Accepted January 17, 2025

Introduction

Parkinson's disease (PD) is the second most common neurodegenerative disease affecting approximately 1-2% of the population over 60 years of age (1). The clinical symptoms of PD is bradykinesia, resting tremor, rigidity, posture instability, and cognitive impairment. Pathologically, symptoms of PD result from a progressive loss of dopaminergic neurons in the substantia nigra (SN) and a following marked reduction in the release of the their neurotransmitter, dopamine (DA) (2, 3). Although the etiopathogenesis of the PD remains unclear, increasing evidences suggests that oxidative stress and neuro-inflammation are the main mechanisms of the dopaminergic neuronal cell loss (4, 5).

The neurotoxin 6-hydroxydopamine (6-OHDA), a hydroxylated analogue of DA, evokes specific neurotoxicity to catecholaminergic (dopaminergic) neurons in the central nervous system (CNS), and for this reason, has been widely used to induce models of PD (6). The selective effect of 6-OHDA has been attributed to its uptake *via* monoamine transporters (7). It has been proposed that the absorbed 6-OHDA causes cytotoxic effect *via* 3 main mechanisms: i) auto-oxidation of 6-OHDA by molecular oxygen to generate hydrogen peroxide, superoxide, and hydroxyl radicals (8); ii) formation of hydrogen peroxide by the monoamine oxidase activity (9); iii) direct inhibition of mitochondrial respiratory chain complex I and IV (10). These mechanisms may act independently or in combination to generate intracellular reactive oxygen species, and increase the cytoplasmic free calcium, and finally induce cell death (11).

Activating transcription factor 3 (ATF3) is a member of the mammalian activating transcription factor (ATF)/cyclic AMP responsive element-binding protein (CREB) family of transcription factors (12). It is rapidly induced by a wide-range of cellular stresses, including DNA damage, oxidative stress, and endoplasmic reticulum stress, and plays an important role in maintaining the cell homeostasis by activating the cell signaling cascades (13). ATF3 has been also proposed as a sensitive marker for neuronal stress and/or injury because it is not normally expressed in healthy neurons but is highly expressed in neuronal cells in response to axotomy (14), ischemia (15), traumatic brain injury (16), toxicity (17), and seizure (18). ATF3 has been implicated in both neuroprotective and detrimental roles, depending on cell type, cellular environment and context of expression (13, 14, 17).

Galectins are an evolutionary conserved family of β-galactoside-binding lectins, sharing a common structural fold and at least one conserved carbohydrate recognition domain of the carbohydrate-binding site (19). Galectins show wide range of biological expression in various tissues among different species, not only in vertebrates but also in invertebrates (19). In mammalian tissues, fifteen galectins have been established so far, which are classified into three (proto, chimera, and tandem repeat) types based on their structures (20). Galectin-3 (Gal3) is one of the most studied one of the galectin family and it is predominantly located in the cytoplasm and sometimes shuttles into the nucleus. It also can be transported to the cell surface and secreted into the interstitial spaces of the tissues or into the biological fluids (21). Several pivotal roles of intracellular Gal3 have been proposed, including mRNA splicing (22, 23), pro- or anti-apoptotic processes (24), molecular tracking (25), and regulation of gene expression (26). Meanwhile, cell surface or extracellular Gal3 plays important roles as a proinflammatory mediator through binding to the microbial pathogens, as well as through recruitment and activation of immune cells (27, 28).

In CNS, Gal3 has been proposed to be involved in neurodevelopment, neuroinflammation, and neurodegeneration (29). More specifically, Gal3 has been shown to influence the migration and differentiation of neuroblasts and neuroglia (30, 31). Gal3 also deems to be one of the key factors in neuroglial, especially microglial, activation (32), and can involve inflammatory response in the CNS by modulating the expression of pro-inflammatory cytokines, such as interleukin 4 (IL-4), IL-17, interferon-γ, and tumor necrosis factor-α (33, 34). There is also accumulating evidences that Gal3 is implicated in neurodegenerative diseases such as Alzheimer's disease (AD), PD, and

Huntington's disease (HD) (20). However, the role of Gal3 in PD is yet to be elucidated.

The primary goal of this study was to determine whether Gal3 expression in SN dopaminergic neurons is selectively affected by 6-OHDA neurotoxicity. The secondary goal of this study was to demonstrate the co-expression of Gal3 with ATF3 in the SN dopaminergic neurons that are immunopositive for FG, *i.e.*, neurons that have been retrogradely insulted with 6-OHDA by means of triple-immunofluorescent labeling. These results will open new and early roles of Gal3 in the 6-OHDA induced PD pathogenesis.

Materials and Methods

Animals. Adult male Wistar rats (n=30, 8 weeks old, Charles River Laboratories, Wilmington, MA, USA) weighing 270±20 g were purchased from SamTako Bio Korea (Osan, Republic of Korea). Rats were maintained in a controlled environment with a 12-h light–dark cycle, with ambient room temperature of 20 to 24˚C, and humidity of 55%±10. They had ad libitum access to food and water. All experimental procedures performed on the animals were approved by the Animal Review Board of Eulji University in accordance with the National Institutes of Health Guide for the Care and Use of Laboratory Animals (NIH Publication No. 80–23, revised 1996).

FG and 6-OHDA administration. Rats were anesthetized *via* intraperitoneal injection of ketamine (70 mg/kg; Yuhan corporation, Seoul, Republic of Korea) and xylazine (Rompun, 8 mg/kg; Bayer Korea Co., Seoul, Republic of Korea). Following deep anesthesia induction, rats were placed in a stereotaxic instrument (KOPF stereotaxic, Tujunga, CA, USA), and their heads fixed using auditory bars. A midline incision was made from the frontal bone between the eyes to the occipital bone, approximately 3 cm in length, and the skin retracted to expose the skull. Two small holes were made with a dental drill on the skull at 1.0 mm anterior to the bregma and 3.0 mm on either side to the midline. A 26 gauge steel needle attached to a 10 µl Hamilton syringe (Hamilton Co., Reno, NV, USA) was lowered through the holes to a depth of 5.0 mm from the skull. Fluoro-Gold (FG; Fluorochrome Inc., Denver, CO, USA) was dissolved in 0.9% saline and 2 µl of 0.1% of FG was injected into the bilateral target coordinates (striatum). The infusion was made using a micro-infusion pump (KD Scientific Inc., Holliston, MA, USA), at a rate of 0.25 µl/min. The needle was left in place for a further 5 min before slowly removing it from the brain parenchyma, and the skin was sutured. After surgery, the animals were kept on a heating pad at 37˚C till the recovery was complete.

On day 3 after bilateral injection of FG, the experimental animals were reanesthetized and 20 µg of 6-OHDA (Sigma-Aldrich, St. Louis, MO, USA) dissolved in 4 µl of 0.2 mg/ml ascorbate-saline was administered. The concentration was based upon previous dose-response studies of 6-OHDA (35-37). The surgical procedures, stereotactic coordinates, and infusion rate of 6-OHDA were performed in the same manner as FG injection. However, 6-OHDA was only administered into the right brain parenchyma. Rats were sacrificed at 1, 3, 5, and 7 days after 6-OHDA injection. The left side of the brains were used as internal controls. Sham-operated animals received 2 µl of 0.2 mg/ml ascorbate-saline.

Tissue preparation. Rats were anesthetized in the same way as surgical procedures and transcardially perfused with physiological saline, followed by 400 ml of 4% paraformaldehyde in phosphate–buffered saline (PBS). The brains were removed carefully and placed on a Rat Brain Blocker (David Kopf Instruments, Tujunga, CA, USA) and then sliced into 10-mm-coronal blocks that included the SN, according to the rat brain atlas (38). They were post-fixed for 2 h in the same fixative and infiltrated with 30% sucrose solution for 12 h at 4˚C until they sank. The sliced blocks were frozen rapidly in 2-methylbutane chilled on dry ice and mounted in Tissue-Tek OCT compound (Sakura Finetechnical Co., Tokyo, Japan). Serial coronal sections of 40 µm thickness were obtained on a Cryostat Microtome (Leica Microsystems Inc., Wetzlar, Germany). Every fourth section was collected at a periodicity of 160

Table I. *The list of primary antibodies used in this study.*

Antibody	Catalog number	Manufacturer	Host	Description	Concentration	
					IHC	IF
Gal3	AF-1197	R&D system	Goat	Wide range of cell type	1:500	1:50
ATF3	Sc-188	Santa Cruz	Rabbit	Wide range of cell type	1:1000	1:100
TH	MAB5280	Millipore	Mouse	Tyrosine hydroxylase	1:1000	1:500
Iba1	AB283319	Abcam	Mouse	Microglia marker		1:200
GFAP	AB279289	Abcam	Mouse	Astrocyte marker		1:200
FG	AB153	Millipore	Rabbit	Fluorogold	1:500	1:100

Gal3, Galectin 3; ATF3, activating transcription factor 3; TH, tyrosine hydroxylase; Iba1, ionized calcium-binding adapter molecule 1; GFAP, glial fibrillary acidic protein; FG, fluorogold; IHC, immunohistochemistry; IF, immunofluorescence.

μm as one set, so eight sets of coronal brain sections were prepared for each animal brain sliced block.

Immunohistochemistry. Tissue sections were washed for 10 min in 0.1 M PBS and endogenous peroxidase activity was quenched by incubating them with 0.3% hydrogen peroxide in PBS for 30 min. Then, they were rinsed in PBS and incubated in PBS containing 10% normal serum from the same host species as the secondary antibody and 0.1% Triton X-100 for 1 h to reduce non-specific staining. The sections were incubated with primary antibodies, which were diluted in 0.1 M PBS containing 0.1% Triton X-100 (PBS-T), at 4˚C overnight. The information of the primary antibodies used in this study are summarized in Table I. The sections were washed three times with PBST and incubated with the appropriate secondary antibodies: biotinylated donkey anti-goat immunoglobulin G (IgG) (1:200; Vector Labs, Burlingame, CA, USA) for Gal3, biotinylated horse anti-rabbit IgG (1:200; Vector Labs) for FG and ATF3, and biotinylated horse anti-mouse IgG (1:200; Vector Labs) for TH. After a 2- h incubation, the sections were washed and sequentially incubated with an Avidin-Biotin Peroxidase Complex (Vector Labs) for 1 h. Antigens were visualized with 3,3′-diaminobenzidine tetrahydrochloride (DAB; Sigma-Aldrich) solution containing 0.003% hydrogen peroxide. Sections were mounted on gelatin-coated slides, dehydrated through a graded ethanol series, cleared in xylene, and coverslipped with Permount (Fisher Scientific, Pittsburgh, PA, USA). The specificity of the immunolabeling was validated by omitting the primary antibodies. To exclude possible confounding results in the quantitative analysis, immunohistochemical procedures were processed in keeping strictly to defined incubation times and reaction condition.

Immunofluorescence. Double immunofluorescence labeling for Gal3/TH, Gal3/GFAP, Gal3/Iba1 and ATF3/TH, ATF3/GFAP, ATF3/Iba1 was conducted to examine which cell types express Gal3 or ATF3 in the PD model. Following incubation in PBS containing 10% normal donkey serum for 30 min, sections were incubated for 16 h at 4˚C with Gal3 antibody diluted to 1:50 in PBS or ATF3 antibody diluted to 1:100 in PBS. After washing with PBS, FITC-conjugated donkey anti-goat IgG (1:200; Jackson ImmunoResearch Labs., West Grove, PA, USA) for Gal3 and a FITC-conjugated donkey anti-rabbit IgG (1:200; Jackson) for ATF3 were applied for 2 h at room temperature in the dark. Following rinse, sections were incubated with TH (nigral dopaminergic marker), Iba1 (microglia marker), and GFAP (astrocytes marker) antibodies, respectively, for 16 h at 4˚C, followed by Cy3-conjugated donkey anti-mouse IgG (1:200; Jackson) for 2h.

We also performed TH/FG double immunofluorescence labeling to determine whether FG administered into the striatum migrated retrogradely and labeled nigral dopaminergic neurons. Brain sections were blocked in PBS with 10% normal donkey serum for 30 min, incubated overnight at 4˚C with a mixture of mouse monoclonal

antibodies against TH (1:500), or rabbit polyclonal antibodies against FG (1:100). After three 10-minute washes in PBS, sections were incubated in a mixture of Cy3-conjugated donkey anti-mouse IgG (1:200; Jackson) and AMCA-conjugated donkey anti-rabbit IgG (1:200; Jackson) for 2 h.

For FG/Gal3/ATF3 triple labeling, sections were incubated with PBS containing 10% normal donkey serum 30 min, followed by the application of the mixture of Gal3 (1:50), ATF3 (1:100) antibodies for 16 h at 4˚C. After three 10-minute washes in PBS, sections were incubated in a mixture of FITC-conjugated donkey anti-goat IgG and Cy3-conjugated donkey anti-rabbit IgG (1:200; Jackson) for 2 h. FG was visualized using a wide band ultraviolet excitation filter, because FG has auto-fluorescence properties.

After immunofluorescence staining, brain sections were mounted on gelatin-coated slides and cover-slipped with Vector-shield medium (Vector). All procedures were conducted in the dark. Control sections were treated similarly except that the primary antibody was omitted to confirm the specificity of the immunofluorescence staining.

Digital photography. Light and fluorescent photomicrographic images were acquired with a LEICA DM6M microscope (Leica microscope system) equipped with appropriate filters and with a LEICA DFC295 digital camera (Leica microscope system). These images were imported into the Adobe Photoshop Software (version 7.0.1; Adobe Systems Inc., San Jose, CA. USA) and were adjusted for brightness and contrast to optimize photographic representation of images obtained by the microscope.

Cell counts. The number of FG-positive, Gal3-positive, and ATF3-positive neurons in the ipsilateral and contralateral SN was counted in 6 animals from each group. From each animal, one set of brain slices that were systematic-randomly sampled between level antero-posterior coordinates -4.5 mm to -6.3 mm to bregma were used. This sampling typically generates around 10 to 11 sections in a series, with 6 sections selected from them. For cell counting, images were acquired of each section scanned under a 200× objective and only the SN region was segmented in the image to measure its area. The borders of the SN at all levels in the rostocaudal axis were defined according to Kirik's method (35). The ventral tegmental area was excluded in this study. The total number of FG-positive, Gal3-positive, and ATF3-positive neurons were counted within a segmented SN region in every section. FG-positive and Gal3-positive neurons were selected for counting only if the entire cell body and highly directed neurites were clearly identified in the image. Since ATF3 signal is localized in the nucleus of the cells and double immunofluorescence results showed that all ATF3 expression was confined in dopaminergic (TH-positive) neurons, the number of ATF3-positive neurons was considered as the number of dots stained for ATF3 in the SN region, To ensure consistency and to escape personal bias, one investigator who was unaware of experimental procedures was responsible for cell counting for the entire study.

Statistical analysis. Data was expressed as the average number (Mean±SEM) of cells per mm^2. Statistical significance was assessed by a one-way ANOVA followed by Bartlett's test using the Prism software (version 6.0; GraphPad Software Inc., San Diego, CA, USA). For all tests, $p \leq 0.05$ was considered significant.

Results

Progressive loss of dopaminergic neurons by 6-OHDA neurotoxicity. Tyrosine hydroxylase immunohisto-chemistry revealed that there was a progressive reduction in the number of TH-positive cells and TH immunoreactivity in the ipsilateral SN, compared to the contralateral counterpart (Figure 1A). Fluorogold immuno-histochemistry also showed progressive loss of FG-positive cells in the ipsilateral SN (Figure 1B). Double immunofluorescence labeling reveled most FG-labeled neurons colocalized with TH-positive neurons (Figure 1C, D). Quantitative assessment of the FG-positive neurons is represented in Figure 1E. The number of FG-positive cells in SN was gradually reduced at 1 day post-lesion (dpl) (185.5±18.09), 3 dpl (105.5±13.26),

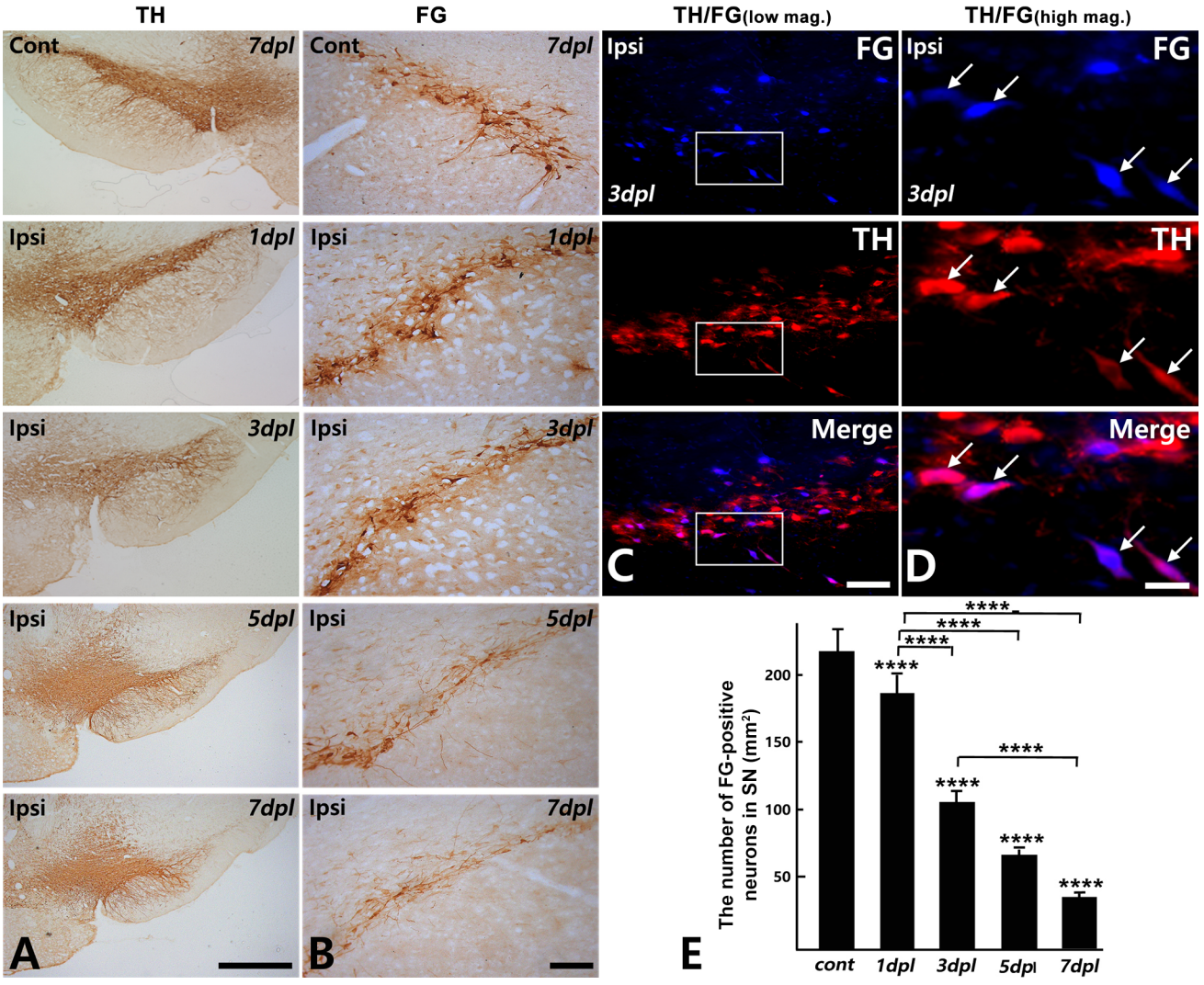

Figure 1. *6-Hydroxydopamine (6-OHDA) induced progressive loss of tyrosine hydroxylase (TH)-positive and fluorogold (FG)-positive neurons in the ipsilateral substantia nigra (SN). (A) Photographs of the TH immunohistochemistry in the contralateral (Cont) and ipsilateral (Ipsi) SN following 6-OHDA lesion. (B) FG immunohistochemistry photographs of the same experimental animals with (A). The TH and FG immunohistochemistry showed a progressive reduction in the number of TH- and FG-positive neurons in the ipsilateral SN. (C) Double immunofluorescence images of TH and FG and their merged image, in the ipsilateral SN at 3 dpl. (D) High magnification image of the area designated by the white square inside of (C). Almost all FG-positive neurons were co-labeled with TH-positive neurons (arrows). (E) Quantitative analysis showing the progressive loss of FG-positive neurons in the SN following 6-OHDA infusion. Scale bars represent 500 μm in (A), 200 μm in (B), 100 μm in (C), and 50 μm in (D). Data are expressed as means±SEM (n=6, *p<0.05; **p<0.01; ***p<0.001; ****p<0.0001). dpl, Days post-lesion.*

5 dpl (66.8±8.42) and 7 dpl (32.0±4.85), compared to the control counterpart (226.5±23.4) in a time-dependent manner. The differences between all groups and the control group were statistically significant (*p<0.05; **p<0.01; ***p<0.001; ****p<0.0001).

Gal3 expression in the ipsilateral nigral dopaminergic neurons. Morphologically typical multipolar neurons (with large cell body and many prominent processes) immunopositive for Gal3 were observed from 1 dpl to the end time point of this experiment (7 dpl) in the ipsilateral

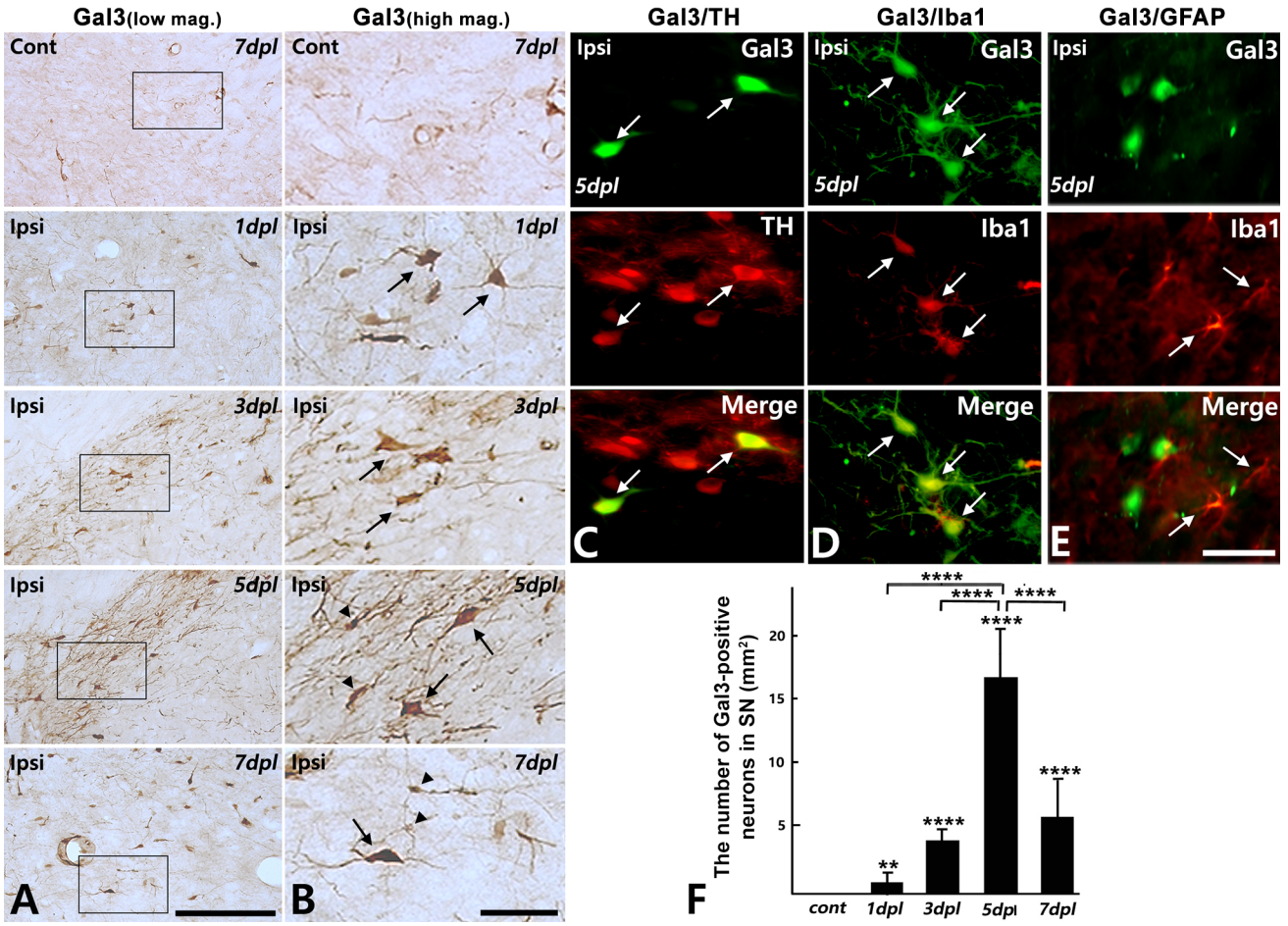

Figure 2. *Gal3 expression was upregulated in the ipsilateral nigral dopaminergic neurons. (A) Photographs of Gal3 immunohistochemistry in the contralateral (Cont) and ipsilateral (Ispi) substantia nigra (SN) after 6-hydroxydopamine (6-OHDA) lesion. Gal3 immunoreactivity was upregulated in the ipsilateral SN. (B) High magnification image of the area designated by the black square inside of (A). Morphologically typical multipolar neurons with large cell body and many prominent processes (arrows) and neuroglia with small cell bodies and many long and slender radiating processes (arrowheads) were positive for Gal3 in the ipsilateral SN. (C) Double immunofluorescence images of Gal3 and TH and their merged image, in the ipsilateral SN at 5 dpl. Gal3 was expressed in many nigral dopaminergic neurons (arrows). (D) Double immunofluorescence images of Gal3 and Iba1 and their merged image. Gal3 was also expressed in many microglial cells (arrows). (E) Double immunofluorescence images of Gal3 and GFAP and their merged image. None of the cells immunolabeled for Gal3 were colocalized with GFAP-positive astrocytes (arrows). (F) Quantitative analysis showing the average number of neurons expressing Gal3 per unit area (mm^2) at each time point. Scale bars represent 200 μm in (A), 50 μm in (B and E). Data are expressed as means±SEM (n=6, *p<0.05; **p<0.01; ***p<0.001; ****p<0.0001). dpl, Days post-lesion.*

SN (Figure 2A and B). Moreover, morphologically typical neuroglia (with small cell bodies and many long and slender radiating processes) immunopositive for Gal3 could be also identified in the ipsilateral SN (Figure 2A and B). In the contralateral SN, few cells were immunopositive for Gal3. To examine which cell types express Gal3, double immunofluorescence staining with Gal3/TH, Gal3/Iba1 (a marker for pan-microglia), and Gal3/GFAP (a marker for astrocytes) was carried out. Morphologically typical multipolar neurons immunopositive for Gal3 were also immunopositive for TH (Figure 2C). Meanwhile, cells immunopositive for Gal3 that were morphologically presumed to be neuroglia colocalized with Iba1 (Figure 2D), but not with GFAP (Figure 2E). Next, we counted the number

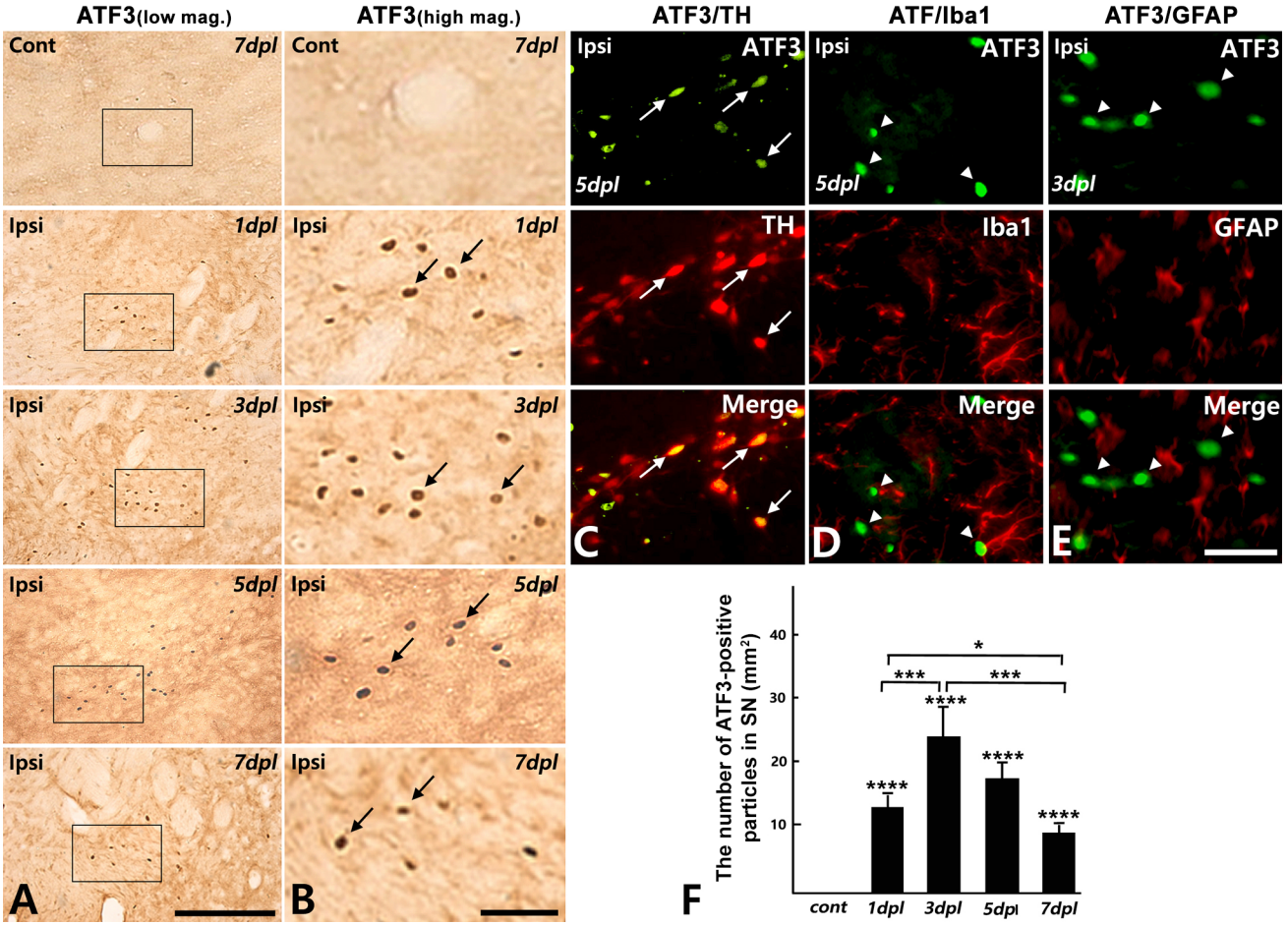

Figure 3. *Concurrent ATF3 expression in the ipsilateral nigral dopaminergic neurons. (A) Photographs of ATF3 immunohistochemistry in the contralateral (Cont) and ipsilateral (Ipsi) substantia nigra (SN) after 6-hydroxydopamine (6-OHDA) lesion. (B) High magnification image of the area designated by the black square inside of (A). ATF3 immunoreactivity was highly upregulated in the ipsilateral SN (arrows). (C) Double immunofluorescence images of ATF3 and TH and their merged image, in the ipsilateral SN at 5 dpl. ATF3 was expressed in the nucleus of the nigral dopaminergic neurons (arrows). (D) Double immunofluorescence images of ATF3 and Iba1 and (E) Double immunofluorescence images of ATF3 and GFAP and their merged image. Neither microglia nor astrocytes express ATF3 [arrowheads in (D) and (E)]. (F) Quantitative analysis showing the average number of neurons expressing ATF3 per unit area (mm^2) at each time point. Scale bars represent 200 μm in (A), 50 μm in (B and E). Data are expressed as means±SEM (n=6, *p<0.05; **p<0.01; ***p<0.001; ****p<0.0001). dpl, Days post-lesion.*

of Gal3 immunolabeled neurons in the ipsilateral SN at each time point. Among those showing Gal3 immuno-reactivity, only cells with definite morphologically multipolar neurons were counted. In the ipsilateral SN, Gal3-positive neurons were first observed at day 1 after 6-OHDA injection (1.8±0.92). Their number was significantly increased on day 3 (4.3±1.85) and peaked on day 5 (16.7±4.68). By day 7 (5.9±3.01), the number of Gal3-positive neurons decreased to a level similar to that on day 3 (Figure 2F).

Concurrent ATF3 expression in the ipsilateral nigral dopaminergic neurons. After unilateral injection of 6-OHDA into the striatum, ATF3 immunopositive small dots were distributed in the ipsilateral SN (Figure 3A, B). There was no ATF3 immunoreactivity in the contralateral SN at any of the experimental time points. To examine which cell types express ATF3 in the ipsilateral SN, we performed double immunofluorescence with antibodies against ATF3/TH, ATF3/Iba1, or ATF3/GFAP. Almost all

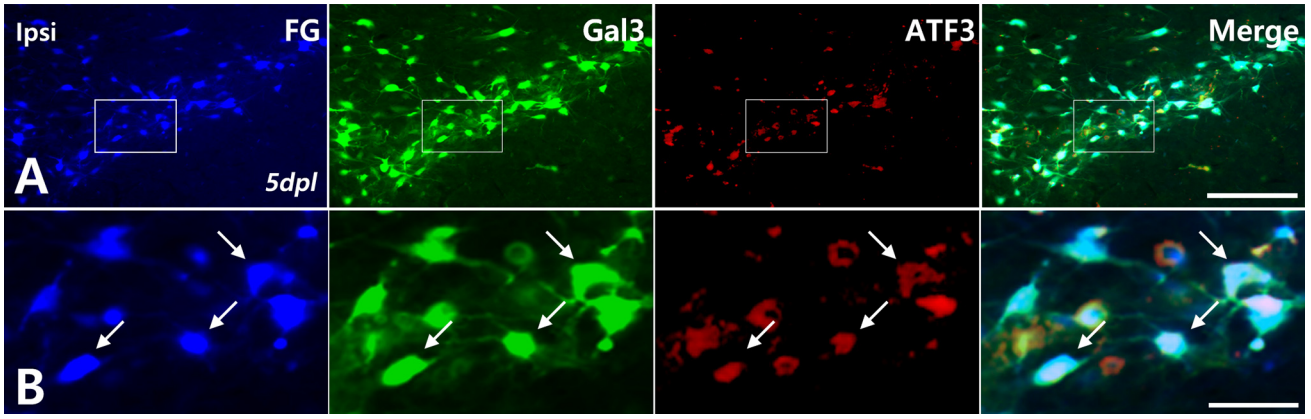

Figure 4. *Co-localization of Gal3 and ATF3 in the 6-OHDA insulted dopaminergic neurons. (A) Representative photomicrographs showing triple immunofluorescence labeling for FG, Gal3, and ATF3 and their merged image in the ipsilateral SN after 6-OHDA lesion at 5 dpl. (B) High magnification image of the area designated by the white square inside of (A). ATF3 and Gal3 were colocalized in the dopaminergic neurons that are labeled with FG, i.e., neurons that have been retrogradely insulted with 6-OHDA. Scale bar represents 200 μm and 50 μm in (A) and (B), respectively. dpl, Days post-lesion; Ipsi, ipsilateral.*

ATF3-positive nuclei were colocalized with TH-positive cells (Figure 3C). Neither GFAP nor Iba1 colocalized with ATF3 (Figure 3D and E). In quantitative analysis, the number of ATF3-positive dots was identified at 1 dpl (12.3±3.46) and peaked at 3 dpl (23.0±5.98). Since then, the number of cells expressing ATF3 has gradually decreased (5 dpl; 18.3±3.48, 7 dpl; 7.65±2.73) (Figure 3F).

Co-localization of Gal3 and ATF3 in the 6-OHDA insulted dopaminergic neurons. Triple immunofluorescence labeling of FG, ATF3, and Gal3 revealed that Gal3 expression and ATF3 expression occurred concomitantly in the FG-labeled neurons (Figure 4).

Discussion

The neurotoxin 6-OHDA has been most widely used to induce animal models of PD since Ungerstedt demonstrated degeneration of the nigrostriatal pathway after intracerebral stereotactic injection of 6-OHDA (39). To assess the degenerative effects and mechanisms of 6-OHDA *in vivo*, three types of 6-OHDA model have been used: i) injection into the medial forebrain bundle (MFB) (40), ii) direct injection into the SN (41), and iii) injection into the striatum (35). Direct lesions into the MFB or parenchymal SN generally result in rapid loss of nigral dopaminergic neurons. In particular, SN lesions can be accompanied by direct mechanical damage to the DA neurons in SN. Meanwhile, unilateral intrastriatal injection of 6-OHDA induce progressive damage to the dopaminergic neurons in SN, thus it is more suitable for studying the degenerating mechanisms underlying 6-OHDA neurotoxicity in the long term (42). Therefore, in this study, we employed unilateral 6-OHDA striatal injection model.

Consistent with previous experimental evidence (35, 36), the unilateral striatal injection of 6-OHDA caused gradual loss of dopaminergic neurons in the ipsilateral SN in a time-dependent manner. The striatum receives afferent fibers from many brain such as cortex, limbic system, SN and ventral tegmental area (VTA). This explains why 6-OHDA lesions on the striatum mainly affect dopaminergic neurons in VTA as well as SN. However, since the loss of dopaminergic neurons in VTA, unlike in the SN, does not exceed 20% and the amount of cell loss does not increase significantly with time (35, 36), we excluded observations and discussion of pathologic changes in dopaminergic neurons in the VTA from this study. Nevertheless, it is worth pointing out that similar results to those observed in SN were also observed in VTA.

To evaluate the loss of dopaminergic neurons in SN and to identify dopaminergic neurons in SN insulted with 6-OHDA, we infused the FG into the striatum at the same stereotactic coordinates 3 days before 6-OHDA injection. FG is a fluorescent dye which is transported along axons from axon terminals towards the cell body (43) and has been known to do not affect the extent of dopaminergic neuronal cell death after 6-OHDA neurotoxicity (44). Since both FG and 6-OHDA retrogradely affect dopaminergic neurons in the SN *via* nigrostriatal fibers, so the distribution of FG-labeled cells can be considered o reflect the proportion of nigral dopaminergic neurons directly affected by 6-OHDA. According to our findings, FG-labeled neurons were located in the typical arrangement expected for the substantia nigra pars compacta (SNc) region comprising of densely packed dopaminergic neurons. Double immunofluorescence with TH and FG showed that almost of all FG labeled cells in SN were also double labeled with TH-positive dopaminergic neurons. Since the injection of 6-OHDA and FG was confined to a narrow region of the striatum, it is reasonable that the number of FG-labeled cells was less than half of the number of TH-positive dopaminergic neurons. The rate of FG-labeled neuronal loss over one week after 6-OHDA injection appeared linear.

A growing body of evidence supports an important role of Gal3 in the development of neurodegenerative diseases including AD, PD, and amyotrophic lateral sclerosis (ALS) (45-47). Here, Gal3-labeled cells appeared in the SNc region at 1 dpl, and their immunoreactivity peaked at 5 dpl. Interestingly, both dopaminergic neurons and neuroglia in the SN, especially microglia, showed immunoreactivity for Gal3. In our previous work, we demonstrated differential expression of Gal3 in neurons and neuroglia depending on the brain regions in normal rat brain, and we showed that in SN, no cell type expressed Gal3 (48). Therefore, it can be inferred that Gal3 expression in the SN is strongly associated with the pathological progression induced by 6-OHDA toxicity. The expression Gal3 in activated microglia has been demonstrated in many other previous reports (32, 33, 45), but Gal3 expression in neurons has not yet been reported.

Similar to the Gal3 expression pattern, ATF3 immunopositive cells were identified only in the SNc region, which is injured by 6-OHDA. The number of cells expressing ATF3 per unit area tended to be slightly higher at each time point than the number of cells expressing Gal3. ATF3 was not expressed in neuroglia (astrocytes or microglia), but was co-expressed on with TH-positive neurons. In normal healthy brain, ATF3 is expressed at a very low level, if at all, but its expression is rapidly upregulated in response to nerve injury. ATF3 expression in neurons has been known to be closely linked to their survival and their axonal regeneration following axotomy (49). However, our previous works have shown that ATF3 expression had a greater susceptibility to dopaminergic neuronal cell death in PD animal models such as 6-OHDA injection model (48) or MFB axotomy model (50). Others have also supported this hypothesis by indicating that ATF3 plays a critical role in 1-methyl-4-phenylpyridinium ion (MPP^+)-induced apoptosis of the differentiated SH-SY5Y human neural cells, in an *in vitro* PD model (51).

Since ATF3 and Gal3 were both expressed in dopaminergic neurons located in the same SNc region, we investigated the co-localization of ATF3 and Gal3 by double immunofluorescence labeling. Because FG emits blue fluorescence on its own, labeling Gal3 with green fluorescence and ATF3 with red fluorescence will allowed us to determine whether these three fluorophores are emitting light in the same cell.

DA is one of the important neurotransmitters that constitutes the mesolimbic and mesostriatal neural circuits in our brain which plays a key role in reward system and motor modulation. In the process of oxidation of DA to form neuromelanin, DA may readily oxidize non-enzymatically to both 6-OHDA and related quinones (52). Thus, as a theoretical possibility, increased endogenous 6-OHDA could cause oxidative stress and mitochondrial dysfunctions on nigral dopaminergic neurons, ultimately leading to neuronal death. This hypothesis for the role of endogenous 6-OHDA in PD pathophysiology is supported

by the report that a progressive linear loss of dopaminergic neurons occurs per every decade of aging (53) and the fact that PD patients worldwide increase rapidly after age 65, worldwide. Furthermore, reports of the presence of elevated levels of 6-OHDA in postmortem PD brains (54) and urine samples (55) of PD patients treated with long-term levodopa were also noteworthy. Therefore, 6-OHDA may represent an endogenous toxin directly or indirectly affecting the degeneration of nigral dopaminergic neurons in the human brain, and thus elucidating the mechanism of response of nigral dopaminergic neurons to 6-OHDA may provide a crucial step in understanding the pathophysiology of human PD and developing new therapeutic strategy.

Recent clinical studies have shown higher serum level of Gal3 in idiopathic PD patients than in healthy people and a precise correlation between Gal3 serum level and disease progression, suggesting that serum levels of Gal3 can be used as a biomarker for PD diagnosis (56, 57). However, Gal3 up-regulation in the brain and serum has also been reported in patients with several other neurodegenerative diseases, including AD, Huntington's disease (HD), ALS, multiple sclerosis, traumatic brain injury, and stroke (58). Therefore, it is reasonable to infer that Gal3 up-regulation is related to the microglial activation in response to a general neuroinflammatory response, rather than a selective response to a specific neurodegenerative disorders. On the other hand, the most notable finding of this study is that Gal3 expression was up-regulated in nigral dopaminergic neurons in response to 6-OHDA neurotoxicity, which has not been reported elsewhere.

Conclusion

The expression of Gal3 and ATF3 is specifically upregulated in nigral dopaminergic neurons damaged by 6-OHDA. This provides the first *in vivo* evidence that Gal3 is expressed in dopaminergic neurons injured by 6-OHDA. Further studies are needed to investigate the intimate involvement of Gal3 in dopaminergic neuronal cell death.

Funding

This research was supported by the Mid-Career Research Program through the National Research Foundation of Korea (NRF-2020R1C1C1003222) and Electronics and Telecommunications Research Institute (ETRI) of Republic of Korea, grant number 23YS1110.

Conflicts of Interest

This work has been funded by Korea government. The funders had no role in the design of the study; the collection, analysis, or interpretation of the data; the writing of the manuscript; or the decision to submit the manuscript for publication. The Authors declare no financial competing interests or non-financial competing interests.

Authors' Contributions

HIY and DYS designed the study. EJL and YJC performed the experiments. RSW and TKB collected the data and analyzed them. HIY and DYS confirm the authenticity of all the raw data. EJL and YJC wrote the manuscript. HIY and DYS edited the manuscript. All Authors have read and approved the final manuscript.

References

1 Armstrong MJ, Okun MS: Diagnosis and treatment of Parkinson disease. JAMA 323(6): 548, 2020. DOI: 10.1001/jama.2019.22360
2 Fahn S: The 200-year journey of Parkinson disease: Reflecting on the past and looking towards the future. Parkinsonism Relat Disord 46(S1): S1-S5, 2018. DOI: 10.1016/j.parkreldis.2017.07.020
3 Respondek G, Stamelou M, Höglinger GU: Classification of atypical parkinsonism per pathology *versus* phenotype. Int Rev Neurobiol 149: 37-47, 2019. DOI: 10.1016/bs.irn.2019.10.003
4 Blesa J, Trigo-Damas I, Quiroga-Varela A, Jackson-Lewis VR: Oxidative stress and Parkinson's disease. Front Neuroanat 9: 91, 2015. DOI: 10.3389/fnana.2015.00091
5 Niranjan R: Recent advances in the mechanisms of neuroinflammation and their roles in neurodegeneration. Neurochem Int 120: 13-20, 2018. DOI: 10.1016/j.neuint.2018.07.003

6 Simola N, Morelli M, Carta AR: The 6-hydroxydopamine model of Parkinson's disease. Neurotox Res 11(3-4): 151-167, 2007. DOI: 10.1007/BF03033565

7 Glinka Y, Gassen M, Youdim MB: Mechanism of 6-hydroxydopamine neurotoxicity. J Neural Transm Suppl 50: 55-66, 1997. DOI: 10.1007/978-3-7091-6842-4_7

8 Blum D, Torch S, Lambeng N, Nissou M, Benabid AL, Sadoul R, Verna JM: Molecular pathways involved in the neurotoxicity of 6-OHDA, dopamine and MPTP: contribution to the apoptotic theory in Parkinson's disease. Prog Neurobiol 65(2): 135-172, 2001. DOI: 10.1016/S0301-0082(01)00003-X

9 Cohen G, Farooqui R, Kesler N: Parkinson disease: a new link between monoamine oxidase and mitochondrial electron flow. Proc Natl Acad Sci U S A 94(10): 4890-4894, 1997. DOI: 10.1073/pnas.94.10.4890

10 Glinka YY, Youdim MB: Inhibition of mitochondrial complexes I and IV by 6-hydroxydopamine. Eur J Pharmacol 292(3-4): 329-332, 1995. DOI: 10.1016/0926-6917(95)90040-3

11 Singh S, Kumar S, Dikshit M: Involvement of the mitochondrial apoptotic pathway and nitric oxide synthase in dopaminergic neuronal death induced by 6-hydroxydopamine and lipopolysaccharide. Redox Rep 15(3): 115-122, 2010. DOI: 10.1179/174329210X12650506623447

12 Hai T, Wolfgang CD, Marsee DK, Allen AE, Sivaprasad U: ATF3 and stress responses. Gene Expr 7(4-6): 321-335, 1999.

13 Rohini M, Haritha Menon A, Selvamurugan N: Role of activating transcription factor 3 and its interacting proteins under physiological and pathological conditions. Int J Biol Macromol 120(Pt A): 310-317, 2018. DOI: 10.1016/j.ijbiomac.2018.08.107

14 Wong AW, Osborne PB, Keast JR: Axonal injury induces ATF3 in specific populations of sacral preganglionic neurons in male rats. Front Neurosci 12: 766, 2018. DOI: 10.3389/fnins.2018.00766

15 Song DY, Oh KM, Yu HN, Park CR, Woo RS, Jung SS, Baik TK: Role of activating transcription factor 3 in ischemic penumbra region following transient middle cerebral artery occlusion and reperfusion injury. Neurosci Res 70(4): 428-434, 2011. DOI: 10.1016/j.neures.2011.05.002

16 Greer JE, McGinn MJ, Povlishock JT: Diffuse traumatic axonal injury in the mouse induces atrophy, c-Jun activation, and axonal outgrowth in the axotomized neuronal population. J Neurosci 31(13): 5089-5105, 2011. DOI: 10.1523/JNEUROSCI.5103-10.2011

17 Takarada T, Kou M, Hida M, Fukumori R, Nakamura S, Kutsukake T, Kuramoto N, Hinoi E, Yoneda Y: Protective upregulation of activating transcription factor-3 against glutamate neurotoxicity in neuronal cells under ischemia. J Neurosci Res 94(5): 378-388, 2016. DOI: 10.1002/jnr.23723

18 Pernhorst K, Herms S, Hoffmann P, Cichon S, Schulz H, Sander T, Schoch S, Becker AJ, Grote A: TLR4, ATF-3 and IL8 inflammation mediator expression correlates with seizure frequency in human epileptic brain tissue. Seizure 22(8): 675-678, 2013. DOI: 10.1016/j.seizure.2013.04.023

19 Rabinovich GA, Baum LG, Tinari N, Paganelli R, Natoli C, Liu FT, Iacobelli S: Galectins and their ligands: amplifiers, silencers or tuners of the inflammatory response? Trends Immunol 23(6): 313-320, 2002. DOI: 10.1016/s1471-4906(02)02232-9

20 Nio-Kobayashi J, Itabashi T: Galectins and their ligand glycoconjugates in the central nervous system under physiological and pathological conditions. Front Neuroanat 15: 767330, 2021. DOI: 10.3389/fnana.2021.767330

21 Dong R, Zhang M, Hu Q, Zheng S, Soh A, Zheng Y, Yuan H: Galectin-3 as a novel biomarker for disease diagnosis and a target for therapy (Review). Int J Mol Med 41(2): 599-614, 2018. DOI: 10.3892/ijmm.2017.3311

22 Fritsch K, Mernberger M, Nist A, Stiewe T, Brehm A, Jacob R: Galectin-3 interacts with components of the nuclear ribonucleoprotein complex. BMC Cancer 16: 502, 2016. DOI: 10.1186/s12885-016-2546-0

23 Coppin L, Vincent A, Frénois F, Duchêne B, Lahdaoui F, Stechly L, Renaud F, Villenet C, Van Seuningen I, Leteurtre E, Dion J, Grandjean C, Poirier F, Figeac M, Delacour D, Porchet N, Pigny P: Galectin-3 is a non-classic RNA binding protein that stabilizes the mucin MUC4 mRNA in the cytoplasm of cancer cells. Sci Rep 7: 43927, 2017. DOI: 10.1038/srep43927

24 Ruvolo PP: Galectin 3 as a guardian of the tumor microenvironment. Biochim Biophys Acta 1863(3): 427-437, 2016. DOI: 10.1016/j.bbamcr.2015.08.008

25 Bänfer S, Schneider D, Dewes J, Strauss MT, Freibert SA, Heimerl T, Maier UG, Elsässer HP, Jungmann R, Jacob R: Molecular mechanism to recruit galectin-3 into multivesicular bodies for polarized exosomal secretion. Proc Natl Acad Sci U.S.A. 115(19): E4396-E4405, 2018. DOI: 10.1073/pnas.1718921115

26 Gál P, Vasilenko T, Kováč I, Čoma M, Jakubčo J, Jakubčová M, Perželová V, Urban L, Kolář M, Sabol F, Luczy J, Novotný M, Majerník J, Gabius HJ, Smetana KJ: Human galectin-3: Molecular switch of gene expression in dermal fibroblasts *in vitro* and of skin collagen organization in open wounds and tensile strength in incisions *in vivo*. Mol Med Rep 23(2): 99, 2021. DOI: 10.3892/mmr.2020.11738

27 Díaz-Alvarez L, Ortega E: The many roles of galectin-3, a multifaceted molecule, in innate immune responses against pathogens. Mediators Inflamm 2017: 9247574, 2017. DOI: 10.1155/2017/9247574

28 Hatanaka O, Rezende CP, Moreno P, Freitas Fernandes F, Oliveira Brito PKM, Martinez R, Coelho C, Roque-Barreira MC, Casadevall A, Almeida F: Galectin-3 inhibits paracoccidioides brasiliensis growth and impacts paracoccidioidomycosis through multiple mechanisms. mSphere 4(2): e00209-19, 2019. DOI: 10.1128/mSphere.00209-19

29 Srejovic I, Selakovic D, Jovicic N, Jakovljević V, Lukic ML, Rosic G: Galectin-3: Roles in neurodevelopment, neuroinflammation,

and behavior. Biomolecules 10(5): 798, 2020. DOI: 10.3390/biom10050798
30 Comte I, Kim Y, Young CC, van der Harg JM, Hockberger P, Bolam PJ, Poirier F, Szele FG: Galectin-3 maintains cell motility from the subventricular zone to the olfactory bulb. J Cell Sci 124(Pt 14): 2438-2447, 2011. DOI: 10.1242/jcs.079954
31 Pasquini LA, Millet V, Hoyos HC, Giannoni JP, Croci DO, Marder M, Liu FT, Rabinovich GA, Pasquini JM: Galectin-3 drives oligodendrocyte differentiation to control myelin integrity and function. Cell Death Differ 18(11): 1746-1756, 2011. DOI: 10.1038/cdd.2011.40
32 Rahimian R, Béland LC, Sato S, Kriz J: Microglia-derived galectin-3 in neuroinflammation; a bittersweet ligand? Med Res Rev 41(4): 2582-2589, 2021. DOI: 10.1002/med.21784
33 Jiang HR, Al Rasebi Z, Mensah-Brown E, Shahin A, Xu D, Goodyear CS, Fukada SY, Liu FT, Liew FY, Lukic ML: Galectin-3 deficiency reduces the severity of experimental autoimmune encephalomyelitis. J Immunol 182(2): 1167-1173, 2009. DOI: 10.4049/jimmunol.182.2.1167
34 Rahimian R, Lively S, Abdelhamid E, Lalancette-Hebert M, Schlichter L, Sato S, Kriz J: Delayed galectin-3-mediated reprogramming of microglia after stroke is protective. Mol Neurobiol 56(9): 6371-6385, 2019. DOI: 10.1007/s12035-019-1527-0
35 Kirik D, Rosenblad C, Björklund A: Characterization of behavioral and neurodegenerative changes following partial lesions of the nigrostriatal dopamine system induced by intrastriatal 6-hydroxydopamine in the rat. Exp Neurol 152: 259-277, 1998. DOI: 10.1006/exnr.1998.6848
36 Oiwa Y, Sanchez-Pernaute R, Harvey-White J, Bankiewicz KS: Progressive and extensive dopaminergic degeneration induced by convection-enhanced delivery of 6-hydroxydopamine into the rat striatum: a novel rodent model of Parkinson disease. J Neurosurg 98(1): 136-144, 2003. DOI: 10.3171/jns.2003.98.1.0136
37 Yoo HI, Ahn GGY, Lee EJ, Kim EG, Hong SY, Pack SJ, Woo RS, Baik TK, Song DY: 6-Hydroxydopamine induces nuclear translocation of apoptosis inducing factor in nigral dopaminergic neurons in rat. Mol Cell Toxicol 13: 305-315, 2017. DOI: 10.1007/s13273-017-0034-5
38 Paxinos G, Watson C: The rat brain in stereotaxic coordinates. San Diego, CA, USA, Academic Press, 1998.
39 Ungerstedt U: 6-Hydroxy-dopamine induced degeneration of central monoamine neurons. Eur J Pharmacol 5(1): 107-10, 1968. DOI: 10.1016/0014-2999(68)90164-7
40 Venero JL, Revuelta M, Cano J, Machado A: Time course changes in the dopaminergic nigrostriatal system following transection of the medial forebrain bundle: detection of oxidatively modified proteins in substantia nigra. J Neurochem 68(6): 2458-2468, 1997. DOI: 10.1046/j.1471-4159.1997.68062458.x
41 Stanic D, Finkelstein DI, Bourke DW, Drago J, Horne MK: Timecourse of striatal re-innervation following lesions of dopaminergic SNpc neurons of the rat. Eur J Neurosci 18(5): 1175-1188, 2003. DOI: 10.1046/j.1460-9568.2003.02800.x
42 Hernandez-Baltazar D, Zavala-Flores LM, Villanueva-Olivo A: The 6-hydroxydopamine model and parkinsonian pathophysiology: Novel findings in an older model. Neuroglia 32(8): 533-539, 2017. DOI: 10.1016/j.nrleng.2015.06.019
43 Ju G, Han Z, Fan Z: Fluorogold as a retrograde tracer used in combination with immunohistochemistry. J Neurosci Methods 29: 69-72, 1989. DOI: 10.1016/0165-0270(89)90109-x
44 Emsley JG, Lu X, Hagg T: Retrograde tracing techniques influence reported death rates of adult rat nigrostriatal neurons. Exp Neurol 168(2): 425-433, 2001. DOI: 10.1006/exnr.2000.7625
45 Nott A, Holtman IR, Coufal NG, Schlachetzki JCM, Yu M, Hu R, Han CZ, Pena M, Xiao J, Wu Y, Keulen Z, Pasillas MP, O'Connor C, Nickl CK, Schafer ST, Shen Z, Rissman RA, Brewer JB, Gosselin D, Gonda DD, Levy ML, Rosenfeld MG, McVicker G, Gage FH, Ren B, Glass CK: Brain cell type-specific enhancer-promoter interactome maps and disease-risk association. Science 366(6469): 1134-1139, 2019. DOI: 10.1126/science.aay0793
46 Boza-Serrano A, Ruiz R, Sanchez-Varo R, García-Revilla J, Yang Y, Jimenez-Ferrer I, Paulus A, Wennström M, Vilalta A, Allendorf D, Davila JC, Stegmayr J, Jiménez S, Roca-Ceballos MA, Navarro-Garrido V, Swanberg M, Hsieh CL, Real LM, Englund E, Linse S, Leffler H, Nilsson UJ, Brown GC, Gutierrez A, Vitorica J, Venero JL, Deierborg T: Galectin-3, a novel endogenous TREM2 ligand, detrimentally regulates inflammatory response in Alzheimer's disease. Acta Neuropathol 138(2): 251-273, 2019. DOI: 10.1007/s00401-019-02013-z
47 Clarke BE, Patani R: The microglial component of amyotrophic lateral sclerosis. Brain 143(12): 3526-3539, 2020. DOI: 10.1093/brain/awaa309
48 Yoo HI, Kim EG, Lee EJ, Hong SY, Yoon CS, Hong MJ, Park SJ, Woo RS, Baik TK, Song DY: Anatomical distribution of galectin-3 in the adult rat brain. J Mol Hist 48(3): 133-146, 2017. DOI: 10.1007/s10735-017-9712-9
49 Hunt D, Raivich G, Anderson PN: Activating transcription factor 3 and the nervous system. Front Mol Neurosci 5: 7, 2012. DOI: 10.3389/fnmol.2012.00007
50 Song DY, Yang YC, Shin DH, Sugama S, Kim YS, Lee BH, Joh TH, Cho BP: Axotomy-induced dopaminergic neurodegeneration is accompanied with c-Jun phosphorylation and activation transcription factor 3 expression. Exp Neurol 209(1): 268-278, 2008. DOI: 10.1016/j.expneurol.2007.09.033
51 Zhao Q, Yang X, Cai D, Ye L, Hou Y, Zhang L, Cheng J, Shen Y, Wang K, Bai Y: Echinacoside protects against MPP(+)-induced neuronal apoptosis *via* ROS/ATF3/CHOP pathway regulation. Neurosci Bull 32(4): 349-362, 2016. DOI: 10.1007/s12264-016-0047-4
52 Napolitano A, Pezzella A, Prota G: New reaction pathways of dopamine under oxidative stress conditions: nonenzymatic iron-assisted conversion to norepinephrine and the

neurotoxins 6-hydroxydopamine and 6,7-dihydroxytetrahydroisoquinoline. Chem Res Toxicol 12(11): 1090-1097, 1999. DOI: 10.1021/tx990079p

53 Fearnley JM, Lees AJ: Ageing and Parkinson's disease: Substantia nigra regional selectivity. Brain 114(Pt 5): 2283-2301, 1991. DOI: 10.1093/brain/114.5.2283

54 Curtius HC, Wolfensberger M, Steinmann B, Redweik U, Siegfried J: Mass fragmentography of dopamine and 6-hydroxydopamine. Application to the determination of dopamine in human brain biopsies from the caudate nucleus. J Chromatogr 99: 529-540, 1974. DOI: 10.1016/s0021-9673(00)90882-3

55 Andrew R, Watson DG, Best SA, Midgley JM, Wenlong H, Petty RKH: The determination of hydroxydopamines and other trace amines in the urine of Parkinsonian patients and normal controls. Neurochem Res 18(11): 1175-1177, 1993. DOI: 10.1007/BF00978370

56 Yazar HO, Yazar T, Cihan M: A preliminary data: Evaluation of serum Galectin-3 levels in patients with Idiopathic Parkinson's Disease. J Clin Neurosci 70: 164-168, 2019. DOI: 10.1016/j.jocn.2019.08.032

57 Cengiz T, Türkboyları S, Gençler OS, Anlar Ö: The roles of galectin-3 and galectin-4 in the idiopatic Parkinson disease and its progression. Clin Neurol Neurosurg 184: 105373, 2019. DOI: 10.1016/j.clineuro.2019.105373

58 García-Revilla J, Boza-Serrano A, Espinosa-Oliva AM, Soto MS, Deierborg T, Ruiz R, de Pablos RM, Burguillos MA, Venero JL: Galectin-3, a rising star in modulating microglia activation under conditions of neurodegeneration. Cell Death Dis 13(7): 628, 2022. DOI: 10.1038/s41419-022-05058-3